The Overexpression of Four MiTFL1 Genes from Mango Delays the Flowering Time in Transgenic Arabidopsis

Yi-Han Wang
Guangxi University
Xin-Hua He
Guangxi University
Hai-Xia Yu
Guangxi University
Xiao Mo
Guangxi University
Yan Fan
Guangxi University
Zhi-Yi Fan
Guangxi University
Xiao-Jie Xie
Guangxi University
Yuan Liu
Guangxi University
Cong Luo (22003luocong@163.com)
Guangxi University

Research Article

Keywords: Mangifera indica L., MiTFL1s, Expression, Function, Protein interactions

Posted Date: March 2nd, 2021

DOI: https://doi.org/10.21203/rs.3.rs-218595/v1

Abstract

Background: *TERMINAL FLOWER 1* (*TFL1*) belongs to the phosphatidylethanolamine-binding protein (PEBP) family, which is involved in inflorescence meristem development and represses flowering in several plant species. In the present study, four *TFL1* genes were cloned from the mango (*Mangifera indica* L.) variety 'SiJiMi' and named *MiTFL1-1*, *MiTFL1-2*, *MiTFL1-3* and *MiTFL1-4*.

Results: A sequence analysis showed that the encoded MiTFL1 proteins contained a conserved PEBP domain and belonged to the TFL1 group. The expression of the *MiTFL1* genes was examined in several tissues, including juvenile leaves, mature leaves, mature stems, and flowers. The highest *MiTFL1* expression level was detected in mature stems followed by juvenile leaves but was lower in mature leaves and flowers during the flowering period. Further expression studies showed that *MiTFL1s* were highly expressed in leaves during the floral induction and differentiation periods. Overexpression of the four *MiTFL1* genes delayed the flowering time in transgenic *Arabidopsis*. The results also showed that *MiTFL1-1* and *MiTFL1-3* could change the flower morphology in some transgenic plants. Yeast two-hybrid analysis showed that several stress-related proteins can interact with MiTFL1s.

Conclusions: Four *MiTFL1* genes exhibit a similar expression pattern, and overexpressed in *Arabidopsis* resulted in delayed flowering. In addition, *MiTFL1-1* and *MiTFL1-3* overexpression affected floral organ development. MiTFL1s can interact with bHLH and 14-3-3 proteins. These results indicate that *MiTFL1s* might play an important role in the flowering process in mango.

Background

Flowering transition is an important stage in the lifecycle of higher plants. The process underlying the flowering transition from the vegetative to reproductive phase is regulated by complex internal signals and external environmental factors [1, 2]. A variety of flowering response pathways, such as photoperiod, vernalization, gibberellin, autonomous, ambient temperature, and age-related pathways, have been identified in the model plant *Arabidopsis thaliana* [3]. Numerous genes play important roles in these processes, and the involved interactions specify the meristem fate [4]. *CONSTANS* (*CO*) contains a zinc finger structure and CCT domain, which activates the *FLOWERING LOCUS T* (*FT*) gene transcribed by binding to the *FT* promoter region, and the *FT* protein moves from the leaf tissue to the stem apex to initiate the transition of the plant from vegetative to reproductive growth [5, 6]. The *FLOWER LOCUS C* (*FLC*) gene plays a central role in vernalization, which refers to the induction of plant flowering [7, 8] and inhibits flowering by binding to *FT*, *FLOWERING LOCUS D* (*FD*) and *SUPPRESSOR OF OVER-EXPRESSION OF CONSTANS1* (*SOC1*) and inhibiting the expression of these genes [9]. The flower meristem-specific genes *LEAFY* (*LFY*) and *APETALA1* (*AP1*) can directly induce shoot apical meristem differentiation, which encourages plants to enter the flowering stage, and are activated by *FT* or *SOC1* [10].

TERMINAL FLOWER 1 (*TFL1*), which belongs to the phosphatidylethano- -lamine-binding protein (PEBP) family, was first identified in *Arabidopsis* [11]. *TFL1* and *FT* are homologous genes with highly

homologous sequences, but their functions are completely opposite. *TFL1* encodes proteins with conserved His88 and Asp144 residues and the typical amino acid triad modules EYD, YFG, and END [12]. The FT protein does not have this structure, which is an important reason for the opposite functions of these two genes [13]. *TFL1* genes, as flowering repressors, determine the timing of the transition of the apical meristem into an inflorescence meristem and the branching pattern of the inflorescence [14]. In *Arabidopsis*, the *AtTFL1* gene not only maintains the infinite growth of the stem apical meristem and inflorescence meristem but is also involved in flower formation [15]. In most fruit trees, the function of *TFL1* homologous genes is delaying flowering, which is similar to the function of *AtTFL1*. For example, the function of *PmTFL1* (*Prunus mume*) is delaying flowering in transformed *Arabidopsis* [16]. The antagonistic effect between *FT* and *TFL1* exhibits a certain relationship with competition with *FD* [17, 18]. The *TFL1* gene inhibits the expression of *LFY* and *AP1*, which are downstream of the *FT* gene, by binding to *FD* and thereby inhibit flowering [19]. Moreover, *LFY* and *AP1* regulate the expression of the *TFL1* gene in opposite manners: *LFY* serves as an activator, *AP1* is a suppressor, and these two genes form an unclear feedback loop. The flowering of plants depends on the ratio of *TFL1* to *LFY* gene expression. A high ratio maintains the plants in a flowering inhibition period, whereas plants with a low ratio are in the early flowering period [20].

Compared with annual plants, woody fruit trees have a longer juvenile period, which seriously affects the process of breeding. Several studies have shown that the overexpression or silencing of flowering-related genes can shorten the juvenile period and promote flowering. For example, the *BpMADS4* gene from silver birch is constitutively overexpressed in apple, and the transgenic plants exhibit markedly shortened juvenile and flowering periods [21]. *PcTFL1-1* and *PcTFL1-2* have been silenced in European pears using RNAi technology, and the plants show early flowering traits and a shortened juvenile period [22].

Mango (*Mangifera indica* L.) is a world-famous woody fruit tree that is widely grown in tropical and subtropical areas. Several environmental factors affect mango flowering, and these include low temperature, water stress, and carbohydrates. The exogenous spraying of potassium nitrate, paclobutrazol and ethephon can promote flowering, whereas the spraying of gibberellin inhibits flowering [23]. In the past few years, several flowering-regulating genes have been isolated and functionally identified in mango, and these include the flowering-promoting gene *MiSOC1* [24], two *MiAP1s* [25], three *MiFTs* [26], and another flowering-suppressing gene (*MiCO*) [27]. The function of *MiTFL1* has not been identified in this plant. In this study, four *MiTFL1* homologous genes, *MiTFT1-1*, *MiTFT1-2*, *MiTFT1-3* and *MiTFT1-4*, were cloned from *M. indica* L. cv. ‘SiJiMi’. The expression patterns of the four *MiTFL1* genes in different tissues and at different flowering development stages were studied. *MiTFL1* gene overexpression vectors were constructed, and the functions of these genes were gained by transformation in *Arabidopsis*. Proteins interacting with MiTFL1 proteins were screened through yeast two-hybrid experiments. This study provides a theoretical basis for shortening the juvenile period of mango and regulating the mango flowering stage.

Results

Isolation and sequences analysis of MiTFL1 genes

Four *TFL1* homologous genes were identified from our previous transcriptome data. We further verified the sequences by RT-PCR and showed that these sequences were consistent with those obtained from the transcriptome data. The four genes were named *MiTFL1-1*, *MiTFL1-2*, *MiTFL1-3* and *MiTFL1-4*, and their DNA sequence lengths were 1175 bp, 1054 bp, 962 bp and 1299 bp, respectively. All *MiTFL1* genes contained four exons and three introns (Fig. 1A). The full coding sequences of the four *MiTFL1s* were 516 bp, 525 bp, 519 bp and 510 bp and encoded 172 aa, 175 aa, 173 aa and 170 aa, respectively. Nucleotide and amino acid sequence alignment analyses showed a higher similarity between *MiTFL1-3* and *MiTFL1-4* (90%) than between *MiTFL1-1* and *MiTFL1-2* (70%). The amino acid sequences of the MiTFL1-1, MiTFL1-2, MiTFL1-3, and MiTFL1-4 proteins exhibited 68.9%, 69.1%, 62.9% and 60.1% similarity with AtTFL1 (NP_196004.1) of *Arabidopsis*, respectively. In addition, all MiTFL1 proteins were identified as TFL1 proteins containing the crucial conserved amino acid residues of TFL1-like proteins (Fig. 1B), namely, histidine at position 85 (H85) and aspartic acid at position 140 (D140).

The PEBP gene family is divided into the *TFL1*, *FT* and *MFT* subfamilies. According to the phylogenetic tree analysis (Fig. 2), the MiTFL1-1, MiTFL1-2, MiTFL1-3 and MiTFL1-4 proteins were clustered with the TFL1 proteins of other species. Among the investigated proteins, the MiTFL1-1 protein was found to be closely related to the TFL1 proteins of apple, pear, apricot, plum, walnut, jujube and other fruit trees of Rutaceae and rose plants. The MiTFL1-2 protein was closely related to the TFL1 proteins of longan and grape and the CEN proteins of apple and cocoa. The MiTFL1-3 and MiTFL1-4 proteins were clustered together and were found to be closely related to the PvCEN protein of pistachio.

Expression analysis of MiTFL1s

The expression pattern of *MiTFL1s* in different tissues of mango, including juvenile leaves, mature leaves, mature stems and flowers, was determined by qRT-PCR (Fig. 3A). The results showed that *MiTFL1-1*, *MiTFL1-2*, *MiTFL1-3* and *MiTFL1-4* were more highly expressed in mature stems than in juvenile leaves and showed lower expression in mature leaves and flowers. *MiTFL1-2* and *MiTFL1-3* exhibited higher expression levels than *MiTFL1-1* and *MiTFL1-4* in all tested tissues.

To explore the expression patterns of the *MiTFL1* genes at different flowering stages of mango, mature leaves of *M. indica* L. cv. ‘SiJiMi’ were collected from the vegetative growth period to the flowering period (November 2016-March 2017), and the results from their analysis are shown in Fig. 3B. The expression patterns of the four *MiTFL1* genes in mature leaves differed among the different flowering stages. *MiTFL1-1* and *MiTFL1-2* were most highly expressed at the flowering induction period (early stage), followed by the floral differentiation period (late stage), whereas the expression level of *MiTFL1-2* was significantly higher than that of *MiTFL1-1*. *MiTFL1-1* and *MiTFL1-2* were expressed at fairly low levels at other flowering development stages. The expression levels of the *MiTFL1-3* and *MiTFL1-4* genes were highest at the floral differentiation period (late stage), followed by the flowering induction period (early stage), and were lower at other stages. Among the tested genes, *MiTFL1-2* presented the highest

expression level at the flowering induction period, and *MiTFL1-3* exhibited the highest expression level at the floral differentiation, inflorescence elongation and flowering periods.

Subcellular localization of MiTFL1s

To examine the subcellular localization of MiTFL1s, 35S::GFP-MiTFL1-1, 35S:: GFP-MiTFL1-2, 35S::GFP-MiTFL1-3, 35S::GFP-MiTFL1-4 and 35S::GFP-P1300 were separately transformed into onion epidermal cells, and the results are shown in Fig. 4. The fluorescent signal of the empty vector 35S::GFP-P1300 was observed in all the cells. The 35S::GFP-MiTFL1-1, 35S::GFP-MiTFL1-2, 35S::GFP-MiTFL1-3, 35S::GFP-MiTFL1-4 fusion proteins were visible only in the nucleus, which was stained with DAPI.

Phenotypic analysis of MiTFL1 overexpression in Arabidopsis thaliana

MiTFL1s delayed flowering in *Arabidopsis thaliana*

To explore the function of the *MiTFL1-1*, *MiTFL1-2*, *MiTFL1-3* and *MiTFL1-4* genes in the flowering process of mango, individual overexpression vectors of pBI121-MiTFL1s were constructed and transferred separately into WT *Arabidopsis thaliana*. Phenotypic observations of T3 generation homozygous plants were conducted, and WT and pBI121 empty vector-expressing *Arabidopsis* served as controls.

Four independent lines of MiTFL1-1-overexpressing (OE-1#13, OE-1#22, OE-1#25 and OE-1#29) and three independent lines of MiTFL1-2-overexpressing (OE-2#24, OE-2#45 and OE-2#55) were selected for functional analysis. Semiquantitative RT-PCR analysis showed that *MiTFL1-1* and *MiTFL1-2* can be expressed normally in the MiTFL1-overexpressing transgenic plants but not in the empty vector-expressing transgenic or WT plants (Figs. 5A1 and 5B1). All independent lines of *MiTFL1-1* and *MiTFL1-2* showed delayed bolting and flowering: these processes occurred at 28.7–32.5 and 33.3–42.2 days, respectively, in these lines and at 24.9–25.3 and 28.5–28.8 days, respectively, in the control plants (Figs. 5A and 5B, Table 1). All transformant lines with *MiTFL1-1* and *MiTFL1-2* showed normal bolting similar to that observed in the WT plants. Additionally, compared the WT plants, the heights of the *MiTFL1-1* and *MiTFL1-2* plants were significantly increased, but the rosette leaves were not significantly affected (Table 1).

Table 1

Flowering phenotype analysis of WT, pBI121, MiTFL1-1-overexpressing (OE-1) and MiTFL1-2-overexpressing (OE-2) transgenic plants

ID	Days to bolting (d)	Days to flowering (d)	No. of rosette leaves	Plant height (cm)
WT	25.3 ± 0.1	28.8 ± 0.2	8.1 ± 0.2	24.1 ± 0.8
pBI121	24.9 ± 0.2	28.5 ± 0.3	7.9 ± 0.2	24.7 ± 0.4
OE-1#13	32.3 ± 0.5*	42.2 ± 1.1*	8.7 ± 0.2	35.7 ± 1.2*
OE-1#22	28.8 ± 0.4*	33.3 ± 0.4*	8.1 ± 0.3	31.9 ± 1*
OE-1#25	29.1 ± 0.6*	33.9 ± 0.5*	8.4 ± 0.3	30.1 ± 0.5*
OE-1#29	28.7 ± 0.4*	33.4 ± 0.6*	8.9 ± 0.3	29.6 ± 0.6*
OE-2#24	31.6 ± 0.5*	37.2 ± 0.7*	8.6 ± 0.3	36.1 ± 1.2*
OE-2#45	32.5 ± 0.3*	38.8 ± 1.2*	8.8 ± 0.3	38.2 ± 1.5*
OE-2#55	29.7 ± 0.3*	34.6 ± 0.5*	8.5 ± 0.3	31.8 ± 1.0*

NOTE: The analysis was performed using four MiTFL1-1-overexpressing and three MiTFL1-2-overexpressing independent transgenic lines. The bolting time and rosette leaves were measured when the bolting height was 0.5-1 cm. The flowering time was considered the time when the first flowers opened. The plant height was measured 15 days after flowering. The error bars represent the ± SDs. The asterisks indicate significant differences (Student's t-test: *P < 0.05).

Three independent lines of MiTFL1-3-overexpressing (OE-3#19, OE-3#23 and OE-3#42) and MiTFL1-4-overexpressing (OE-4#24, OE-4#45 and OE-4#55) were selected for functional analysis. A semiquantitative RT-PCR analysis demonstrated that *MiTFL1-3* and *MiTFL1-4* were abundantly expressed in the transgenic lines but absent in WT and pBI121 transgenic *Arabidopsis* plants (Figs. 6A1 and 6B1). The MiTFL1-3-overexpressing and MiTFL1-4-overexpressing transgenic plants showed normal bolting, but their bolting time was significantly delayed compared with those of the WT and pBI121 transgenic lines under long-day (LD) conditions (Figs. 6A and 6B, Table 2). The inhibitory effect of *MiTFL1-4* on flowering was lower than those of the other three *MiTFL1* genes. The plant heights of some *MiTFL1-3* and *MiTFL1-4* transgenic lines showed significant differences, but the heights of some of the plants did not significantly differ from those of the control lines. The rosette leaves were not significantly affected in any of the plants (Table 2).

Table 2

Flowering phenotype analysis of WT, pBI121, MiTFL1-3-overexpressing (OE-3) and MiTFL1-4-overexpressing (OE-4) plants

ID	Days to bolting (d)	Days to flowering (d)	No. of rosette leaves	Plant height (cm)
WT	24.8 ± 0.3	28.1 ± 0.3	8.1 ± 0.2	24 ± 2.9
pBI121	24.7 ± 0.3	27.4 ± 0.2	8.2 ± 0.4	25.3 ± 0.8
OE-3#19	37.0 ± 0.5*	47.3 ± 0.6*	8.5 ± 0.2	38.9 ± 1.1*
OE-3#23	30.9 ± 0.6*	38.9 ± 1.9*	8.4 ± 0.3	36.1 ± 1.2*
OE-3#42	30.2 ± 0.6*	34.7 ± 0.7*	8.3 ± 0.2	26.3 ± 2.0
OE-4#12	28.0 ± 0.7*	31.8 ± 0.6*	7.6 ± 0.3	26.9 ± 0.7
OE-4#16	26.8 ± 0.3*	30.7 ± 0.3*	8.2 ± 0.2	26.5 ± 0.3
OE-4#24	29.4 ± 0.8*	32.9 ± 0.8*	7.7 ± 0.3	31.2 ± 1.0*

NOTE: The analysis was performed using three MiTFL1-3-overexpressing and three MiTFL1-4-overexpressing independent transgenic lines. The bolting time and rosette leaves were measured when the bolting height was 0.5-1cm. The flowering time was considered the time when the first flowers opened. The plant height was measured 15 days after flowering. The error bars represent the ± SDs. The asterisks indicate significant differences (Student's t-test: *P < 0.05).

MiTFL1-1 and *MiTFL1-3* affect the phenotype of *Arabidopsis*

The MiTFL1-1-overexpressing (Fig. 7B) and MiTFL1-3-overexpressing transgenic lines (Fig. 7C) exhibited similar abnormal phenotypes compared to the WT lines (Fig. 7A). In the transgenic plants, some carpels developed into new inflorescences (Figs. 7B-a and 7C-a), and some flower structures lacked petals (Figs. 7B-b and 7C-b), which was different from the results obtained for the WT plants (Figs. 7A-a and 7A-b). Two types of silique variations were found in the transgenic plants compared with the WT plants (Figs. 7A-b, 7A-c): in some siliques, the fruit stalk continued to lengthen from the flower during formation (Figs. 7B-c and 7C-c), and in other siliques exhibited curved growth and shorter siliques (Figs. 7B-c and 7C-c) compared with those of the WT plants. In addition, the inflorescences of the transgenic plants were also significantly different from those of the WT plants due to the variations in flower morphology (Figs. 7A-d, 7B-e and 7C-e). The results also showed whorled leaves growing on the lateral branches of transgenic Arabidopsis thaliana but not in the control plants (Figs. 7A-e, 7B-f and 7C-f).

Expression patterns of endogenous genes in transgenic *Arabidopsis* expressing *MiTFL1s*

To determine whether *MiTFL1* gene overexpression in transgenic *Arabidopsis* changed the expression of some flowering-related genes, such as *AtFT*, *AtFD*, and *AtAP1* homologue genes in *Arabidopsis*, the aboveground portion of T3 generation homozygous transgenic *Arabidopsis thaliana* was collected 30 days after planting and subjected to qRT-PCR analysis (Fig. 8). *AtACTIN2* was used as the internal reference gene. A similar expression pattern was found for the *AtFT*, *AtFD*, and *AtAP1* transcripts in *Arabidopsis* after the overexpression of each of the four *MiTFL1* genes (Figs. 8A-8D). The expression levels of the *AtFT* and *AtAP1* genes were significantly lower in all *MiTFL1*-overexpressing transgenic lines

than in the WT plants. However, the *AtFD* gene was significantly increased in many transgenic lines with the exception of MiTFL1-2-overexpressing line OE-2#45.

Proteins that interact with MiTFL1s

The yeast two-hybrid system was used to screen the proteins interacting with MiTFL1s and verify their interactions. The bait vector pGBKT7-MiTFL1 was constructed by double enzyme digestion, and no autoactivation or toxicity was detected (shown in Fig. S2). Yeast cells with bait plasmids were combined with the cDNA homogenization library of 'SiJiMi' to screen for the positive clones. Because the yeast two-hybrid system has a high false positive rate, three proteins selected from the library were selected for further point-to-point verification on DDO/X and QDO/X/A media. The three proteins were basic helix-loop-helix protein 13 (bHLH13), bHLH162 and 14-3-3D, as shown in Fig. 9. The cells with the candidate protein bHLH13 in the pGADT7 recombinant vector turned blue and exhibited normal growth on QDO/X/A solid medium, which indicated that the protein interacts with MiTFL1-2 and MiTFL1-3 proteins. bHLH162 can interact with MiTFL1-1, MiTFL1-2 and MiTFL1-4, whereas 14-3-3D only interacts with MiTFL1-1 and MiTFL1-2.

Discussion

FT and *TFL1* encode a pair of flowering regulators belonging to the phosphatidylethanolamine-binding protein (PEBP) family, which play important roles during the switch from vegetative growth to reproductive development [19]. *FT* and *TFL1* share high homology, as demonstrated by high nucleotide and amino acid sequence identities, but have opposite functions. *FT* promotes the transition to reproductive development and flowering, whereas *TFL1* represses flowering [19, 28]. Our previous study identified three *FT* genes from mango and further confirmed that all *FT* genes significantly promoted flowering of the transgenic plants [26]. In the present study, four *TFL1* genes were obtained from 'SiJiMi' mango, and these were named *MiTFL1-1*, *MiTFL1-2, MiTFL1-3* and *MiTFL1-4*. Multiple copies of *TFL1* homologous genes were also found in other plants, such as two in soybean [29], moso bamboo [13] and loquat [30], three in petunia [31], four in cotton [32] and five in *Hevea brasiliensis* [33]. In a previous study, only two *TFL1* genes, *MiTFL1* and *MiTFL1a*, were found in another mango variety, '*Alphonso*', and these corresponded to *MiTFL1-2* and *MiTFL1-1* in the present study, respectively [34]. *MiTFL1* genes contain four exons and three introns. The nucleotide lengths of the second and third exons were highly consistent among different *MiTFL1* genes (Fig. 1A). The key amino acids His88 and Asp144 of TFL1 proteins were also found in these four MiTFL1 proteins (Fig. 1B). The constructed phylogenetic tree indicated that four MiTFL1 proteins belong to the TFL1 protein branch. In the tree, MiTFL1-1 and MiTFL1-2 were close to each other, whereas MiTFL1-3 and MiTFL1-4 were also located close to each other (Fig. 2).

The *TFL1* gene expression pattern is related to the juvenile phase of most fruit trees. The transcriptional accumulation of *CsTFL1* in citrus is positively correlated with the juvenile age [35]. *PmTFL1* of Japanese apricot is expressed in leaves, stems and roots at the juvenile phase, whereas *PmTFL1* has only been detected in leaf buds and young leaves at the mature stage [16]. The *PpTFL1* gene of peach is mainly

expressed in mature young leaves, juvenile leaves and juvenile roots but is not found in mature leaves and flower buds [36]. *EjTFL1-1* is mainly expressed in roots and leaf buds but is expressed at low levels in shoots, flower buds and flowers. *EjTFL1-2* is mainly expressed in leaf buds, flowers, and fruits and is not expressed in the other tissues [30]. In the present study, *MiTFL1* genes showed different expression patterns than those reported above. A tissue expression analysis showed that *MiTFL1-1*, *MiTFL1-2*, *MiTFL1-3* and *MiTFL1-4* presented similar expression patterns and were expressed in both vegetative and reproductive tissues. The highest expression levels were found in the stems and juvenile leaves, whereas lower levels were found in mature leaves, and the lowest levels were observed in flowers. These results were similar to those found for *Prunus serotina PsTFL1* [37] and in another mango variety, '*Alphonso*' [34].

Some studies have shown that the expression pattern of the *TFL1* gene is different at different stages of floral development. For example, in pear, apple, and quince, *TFL1-1* and *TFL1-2* genes are highly expressed in buds before floral differentiation, and their expression appears to decrease after floral differentiation [38]. In *Hevea brasiliensis*, *HbTFL1-1*, *HbTFL1-2* and *HbTFL1-3* expression increases gradually during inflorescence development, but *HbCEN1* and *HbCEN2* continuously decreases over this period [39]. The expression levels of *EjTFL1-1* and *EjTFL1-2* gradually decrease before floral bud differentiation and started to increase again during the flower-opening period [30]. In the mango variety '*Alphonso*', *MiTFL1* expression increases during the flowering induction period and subsequently decreases, whereas *MiTFL1a* expression remains low during the flowering period [34]. In this study, two expression peaks of *MiTFL1* genes were found in mature leaves during flowering development. One of the expression peaks appeared at the flowering induction period (early stage), and the other appeared at the floral differentiation period (late stage). The above-described results showed that the expression patterns of *TFL1* were different in different species or varieties.

TFL1 homologous genes have similar functions in many species, and these functions include delaying the flowering time and maintaining the inflorescence meristem through suppression of the expression of *AP1* and *LFY* [15]. The overexpression of apple *MdTFL1* in *Arabidopsis* delays the flowering time, and inhibition of the expression of the *MdTFL1* gene by RNAi technology results in early flowering traits [33, 40]. Japanese apricot *PmTFL1* [16] and five rubber *TFL1* genes show the same function in transgenic *Arabidopsis* [39]. In the present study, four mango *MiTFL1* genes also had the same function of delayed the flowering time in transgenic *Arabidopsis*. Moreover, the *MiTFL1-1* and *MiTFL1-3* transgenic lines exhibited abnormal flower organ phenotypes, such as missing petals, carpel development into a new inflorescence, curved pod growth and seed abortion. These results suggest that *MiTFL1-1* and *MiTFL1-3* are involved in flower organ development. Similar phenotypes were also found in chrysanthemum *CmTFL1c*- and *Prunus PsTFL1*-overexpressing transgenic *Arabidopsis* lines [37, 41].

Introduction of the exogenous *TFL1* gene significantly downregulated the expression levels of the endogenous genes *AtFT* and *AtAP1* in transgenic *Arabidopsis*, which led to delayed flowering. For example, overexpressing the *HkTFL1* gene in Hemerocallis delayed flowering, and the expression levels of *AtFT* and *AtAP1* in transgenic *Arabidopsis* were decreased compared with those in WT *Arabidopsis* [42].

The *Chrysanthemum morifolium CmTFL1c* gene negatively regulates flowering by inhibiting the expression of *AtFT*, *AtLFY* and *AtAP1* [41]. Cucumber *CsTFL1b* also delays flowering in *Arabidopsis* and decrease and increase the expression levels of *AtFT* and *AtFD*, respectively [4]. In the present study, four *MiTFL1s* downregulated the expression of *AtFT* and *AtAP1* but upregulated the expression of the *AtFD* gene in transgenic *Arabidopsis*.

In rice, the TFL1-like protein RICE CENTRORADIALIS (RCN) can directly interact with the 14-3-3 protein [43]. In this study, 14-3-3 protein D was found to interact with *MiTFL1-1* and *MiTFL1-2*, and this result was similar to that found in rice. Two other bHLH proteins were also found to interact with different MiTFL1 proteins, and the literature suggests that the *bHLH* gene plays a role in several processes, including growth, development, and response to various stresses [44]. The mechanism through which the *TFL1* gene interacts with *bHLH* to regulate plant growth and development needs further research.

Conclusions

In this study, four *MiTFL1* genes were identified in mango. These proteins both contained the key amino acids His88 and Asp144. An expression analysis showed that *MiTFL1s* exhibit a similar expression pattern: *MiTFL1s* are expressed in vegetative and reproductive tissues and highly expressed in mature leaves during the flowering induction period and the floral differentiation stage. Overexpression of the four *MiTFL1* genes in *Arabidopsis* resulted in delayed flowering, whereas *MiTFL1-1* and *MiTFL1-3* overexpression affected floral organ development. The yeast two-hybrid analysis showed that MiTFL1s can interact with bHLH and 14-3-3 proteins. These results provide preliminary evidence showing that *MiTFL1s* negatively regulate floral induction in mango, but their interaction mechanisms need to be further validated.

Methods

Plant materials and growth conditions

The *M. indica* L. cv. SiJiMi’ plants used in this study were planted in the orchard at Guangxi University, Nanning, Guangxi, China (22°502 N, 108°17'E). This cultivar was selected by researchers at Guangxi University. Additionally, it was approved by the Guangxi Variety Examination and Approval Committee in 2011 (Certification number: 2011006). For tissue expression analysis, juvenile leaves were collected from 8-month-old seedlings. Mature leaves, mature stems and flowers were collected from 3-year-old trees on 11 March 2017. For seasonal expression analysis, leaves were collected once per month from 1 November 2016 to 11 March 2017. All the samples were immediately frozen in liquid nitrogen and stored at -80°C. The *Arabidopsis* ecotype Col-0 was obtained from the laboratory of College of Agriculture, Guangxi University

Isolation of MiTFL1s **from mango**

The total RNA of mango leaves was extracted with the RNAprep Pure Plant Kit (TianGen, Beijing, China) according to the instructions. First-strand cDNA was synthesized from 1 μg of total RNA with the M-MLV reverse transcriptase (TaKaRa, Dalian, China) according to the manufacturer's instructions. Genomic DNA was extracted from mango leaves using the CTAB method. Four *TFL1* genes were obtained from mango dates and named *MiTFL1-1*, *MiTFL1-2*, *MiTFL1-3* and *MiTFL1-4*. Specific primers (QTFL1-1u/d, QTFL1-2u/d, QTFL1-3u/d, QTFL1-4u/d and shown in Table S1) were designed to amplify *MiTFL1s* from genomic DNA and cDNA. The polymerase chain reaction (PCR) mixture contained 2.5 μl of 10× PCR buffer (with $MgCl^{2+}$), 0.5 μl of 10 mM dNTPs (Sangon Biotech, Shanghai, China), 1 μl of each of the upstream and downstream primers (10 μM), 0.15 μl of the TransTaq-T DNA polymerase enzyme (TianGen, Beijing, China), 1 μl of genomic DNA (100 ng/μl) or cDNA (100 ng/μl), which served as the templates, and sterile water (25 μl). The PCR amplification conditions included an initial denaturation step of 4 min at 95°C, 38 cycles of 95°C for 40 s and 56°C for 50 s, 72°C for N min (N = 1 min/kp), and a final extension at 72°C for 10 min. The amplified fragments were cloned into the pMD18-T vector (Takara, Dalian, China) and then sequenced.

Sequence analysis

Sequence analysis and amino acid prediction were performed using BioXM 2.6 software. IBS Version 1.0 was used to generate exon-intron structures. The conserved domains were analyzed using the NCBI BLAST search engine (https://www.ncbi.nlm.nih.gov/Structure/cdd/wrpsb.cgi). The amino acid sequences of the FT1/TFL1 family were downloaded through BLAST searches of GenBank (http://www.ncbi.nlm.nih.gov/BLAST/). Multiple sequence alignments of TFL1 proteins were analyzed using DNAMAN software. The phylogenetic tree was constructed using the neighbor-joining method in MEGA 6.0 with 1000 bootstrap replicates.

Expression analysis of MiTFL1s

The expression of *MiTFL1* genes was detected by quantitative real-time PCR. Total RNA of all the samples was extracted using the RNAprep Pure Plant Kit (TianGen, Beijing, China) according to the instructions. First-strand cDNA was synthesized and used as a template. Gene-specific primers (qTFL1-1u/d, qTFL1-2u/d, qTFL1-3u/d and qTFL1-4u/d) were designed to distinguish the *MiTFL1* genes. The *MiActin1* gene of mango was used as the internal reference gene [45]. The PCR mixture contained 10 μl of SYBR Premix Ex Taq II (Takara, Dalian, China), 1 μl of cDNA (100 ng/μl), 0.5 μl (10 μM) of the upstream and downstream primers, 0.8 μl of ROX Reference Dye II, and sterile water to a total volume of 20 μl. The PCR amplification conditions included 30 s at 95°C, 40 cycles of 95°C for 5 s, 60°C for 34 s, and 95°C for 15 s, 60°C for 1 min, and 95°C for 15 s. The relative transcript abundances were estimated using the $2^{-\Delta\Delta Ct}$ method [46]. The analysis of each sample was repeated three times.

Subcellular localization of MiTFL1s

The full coding sequences of *MiTFL1s* without terminator codons were constructed into P1300-GFP vectors with *Xba*I and *BamH*I restriction enzyme cutting sites. The construction vectors were transformed

into *Agrobacterium tumefaciens* EHA105. The GFP fusion vectors and the empty vector were subsequently transformed into onion epidermal cells by *Agrobacterium tumefaciens* EHA105. 4', 6-Diamidino-2-phenylindole (DAPI) was used to visualize the nucleus. Images were captured with a high-resolution laser confocal microscope (TCS-SP8MP, Leica, Germany).

Plasmid construction and genetic transformation

The MiTFL1s-overexpressing (OE) vectors were constructed into pBI121 binary vectors with *Xba*Ⅰ and *Xma*Ⅰ restriction enzyme cutting sites. The overexpression plasmid was transferred into *A. tumefaciens* strain EHA105. All overexpression vectors and the empty vector were subsequently transformed into WT *Arabidopsis thaliana* using the floral-dip method [47]. The transgenic seeds were selected on 1/2 MS medium containing 50 mg/l kalamycin and confirmed by genomic PCR. The specific primers MiTFL1-1u/d, MiTFL1-2u/d, MiTFL1-3u/d and MiTFL1-4u/d were used to detect whether the transformation of *MiTFL1* genes was successful. Homozygous T3 transgenic plants were used for the subsequent experiments.

Phenotypic analyses

Wild-type and empty vector-transformed *Arabidopsis* plants were used as controls. Several phenotypic indexes, including the bolting time, flowering time, time from bolting to flowering, and rosette leaves, were measured. To detect the expression levels of *MiTFL1s* and some flowering-related genes in transgenic and control plants, 30-day-old seedlings of both transgenic and WT *Arabidopsis* plants were collected for total RNA extraction. Total RNA was extracted, and first-strand cDNA was synthesized as described above. Semiquantitative RT-PCR was performed to detect the expression levels of *MiTFL1s* in transgenic and control lines. The PCR amplification conditions consisted of an initial denaturation step of 2 min at 95°C, 30 cycles of 95°C for 30 s, 56°C for 30 s, and 72°C for 30 s, and a final extension of 72°C for 5 min. The PCR products were electrophoretically separated on a 1.8% agarose gel. The expression levels of some endogenous flowering-related genes in transgenic and control *Arabidopsis* lines were detected by qRT-PCR using the reaction system and conditions described above. *Arabidopsis AtACTIN2* was used as the internal reference gene for qRT-PCR analysis. All the primers used in this study are listed in Supplemental Table 1.

Proteins interacting with MiTFL1s

A cDNA library from *M. indica* L. cv. SiJiMi leaves and flowering organs was constructed using the Yeast Two-Hybrid Library Construction Kit (Clontech, Dalian, China). Yeast two-hybrid (Y2H) assays were performed according to the Yeastmaker™ Yeast Transformation System 2 protocol (Clontech, Dalian, China). The full coding sequences of *MiTFL1s* were constructed into the pGBKT7 vector with *Nde*Ⅰ and *EcoR*Ⅰ restriction enzyme cutting sites. The pGBKT7-bait plasmid was transformed into yeast competent Y2H Gold cells, which were diluted 10^{-1} and 10^{-2} and coated on SDO/-Trp, SDO/-Trp/X-alpha-Gal and SDO/-Trp/X-Alpha-Gal/AbA media. The transcriptional activity and toxicity were verified using this method.

The interacting proteins were identified by screening a DNA library on QDO/–Trp/–Leu/–His/–Ade culture medium. The plasmids of the interacting proteins were extracted and used for further verification of their actual interactions. Y2H Gold yeast cells with the pGBKT7-bait plasmid and Y187 yeast cells with the candidate prey were mixed and cultured in liquid medium containing 2×YPDA at 30°C and 200 rpm for 20–24 h. The mixture was then coated on DDO/–Trp/–Leu/X and QDO/X/A media and cultured for 3–5 days. The colonies were blue in the media, which indicated a positive interaction. The AbA concentration was 500 μg/ml, and the X-α-gal concentration was 200 ng/ml. Y2H Gold (pGBKT7-53) and Y187 (pGADT7-T) served as positive controls, and Y2H Gold (pGBKT7-LAM) and Y187 (pGADT7-T) were used as negative controls.

Statistical analysis

SPSS 19.0 statistical software (SPSS Inc., Chicago, IL, United States) was used for the statistical analyses.

Abbreviations

CTAB: Hexadecyltrimethylammonium bromide; qRT-PCR: Quantitative reverse transcription polymerase chain reaction; DAPI: 6-Diamidino-2-phenylindole; X-Alpha-Gal: 5-Bromo-4-chloro-3-indoxyl-α-D-galactopyranoside ; AbA: Aureobasidin A

Declarations

Acknowledgements

Not applicable.

Author contributions

CL and XHH designed and financed this experiment; YHW performed the experiments; HXY, XM, YF, ZYF, XJX, YL helped with the experiments and data analysis. YHW and CL wrote the manuscript. All authors have read and approved the final manuscript.

Disclosures

The authors have no conflicts of interest to declare.

Funding

National Natural Science Foundation of China (31860541 and 31660561), Science and Technology Major Projects of Guangxi (GuiKeAA17204026 and GuiKe AA17204097), State Key Laboratory for Conservation

and Utilization of Subtropical Agro-bioresources□SKLCUSA-c201901□□Innovation Team of Guangxi Mango Industry Project (nycytxgxcxtd- 06-02).

Availability of data and materials

All data generated or analyzed during this study are included in this published article and its supplementary information files.

Ethics approval and consent to participate

All the mango and *Arabidopsis* materials used and analyzed for this study were collected from the College of Agriculture, Guangxi University, Guangxi Nanning, China, which were public and available for non-commercial purpose. This article did not contain any studies with human participants or animals performed by any of the authors

Consent for publication

Not applicable.

Competing interests

The authors declare that they have no competing interests.

References

1. Larsson AS, Landberg K, Meeks-Wagner DR. The *TERMINAL FLOWER2* (*TFL2*) gene controls the reproductive transition and meristem identity in Arabidopsis thaliana. Genetics. 1998;149 (2):597–605.
2. Prudencio AS, Hoeberichts FA, Dicenta F, Martínez-Gómez P, Sánchez-Pérez R. Identification of early and late flowering time candidate genes in endodormant and ecodormant almond flower buds. Tree Physiol. 2020; doi: 10.1093/treephys/ tpaa151
3. He YH. Chromatin regulation of flowering. Trends Plant Sci. 2012;17 (9):556–562.
4. Zhao W, Gu R, Che G, Cheng Z, Zhang X. *CsTFL1b* may regulate the flowering time and inflorescence architecture in cucumber (*Cucumis sativus* L.). Biochem. Biophys. Res. Commun. 2018;499 (2):307–313.
5. Luccioni L, Krzymuski M, Sanchezlamas M, Karayekov E, Cerdán PD, Casal JJ, *CONSTANS* delays *Arabidopsis* flowering under short days. Plant J. 2018;97 (5):923–932.

6. Wells RS, Adal AM, Bauer L, Najafianashrafi E, Mahmoud SS. Cloning and functional characterization of a floral repressor gene from Lavandula angustifolia. Planta. 2020;251:41
7. Sheldon CC, Rouse DT, Finnegan EJ, Peacock WJ, Dennis ES. The molecular basis of vernalization: the central role of *FLOWERING LOCUS C* (*FLC*). Proc. Natl. Acad. Sci. U. S. A. 2000;97 (7):3753–3758.
8. Won SY, Jung JA, Kim JS. Genome-wide analysis of the MADS-Box gene family in Chrysanthemum. Comput Biol Chem. 2021;90:107424.
9. Ream TS, Woods DP, Amasino RM. The molecular basis of vernalization in different plant groups. Proc. Natl. Acad. Sci. U. S. A. 2011;77:105–115.
10. Sharma B, Batz TA, Kaundal R, Kramer EM, Larson RB. Developmental and Molecular Changes Underlying the Vernalization-Induced Transition to Flowering in Aquilegia coerulea (James). Genes. 2019;10 (10):734
11. Shannon S, Meeks-Wagner DR. A Mutation in the Arabidopsis *TFL1* gene affects inflorescence meristem development. Plant cell. 1991;3 (9):877–892.
12. Carmona MJ, Calonje M, Martínez-Zapater JM. The *FT/ TFL1* gene family in grapevine. Plant Mol. Biol. 2007;63 (5):637–650.
13. Yang Z, L. Chen L, Kohnen MV, Xiong B, Zhen X, Liao J, Oka Y, Zhu Q, Gu L, Lin CT, Liu BB. Identification and characterization of the PEBP family genes in Moso Bamboo (Phyllostachys heterocycla). Sci Rep. 2019;9:14998.
14. Liu X, Zhang J, Xie DY, Franks RG, Xiang QJ. Functional characterization of *Terminal Flower 1* homolog in Cornus canadensis by genetic transformation. Plant Cell Rep. 2019;38 (3):333–343.
15. Bradley D, Ratcliffe O, Vincent C, Carpenter R, Coen E. Inflorescence commitment and architecture in Arabidopsis. Science. 1997; 275:80–83.
16. Esumi T, Kitamura Y, Hagihara C, Yamane H, Tao R. Identification of a *TFL1* ortholog in Japanese apricot (Prunus mume Sieb. et Zucc.). Sci. Hortic. 2010;125 (4):608–616.
17. Moraes TS, Dornelas MC, Martinelli AP. *FT/ TFL1*: calibrating plant architecture. Front. Plant Sci. 2019;10:97.
18. Périlleux C, Bouché F, Randoux M, Orman-Ligeza B. Turning meristems into fortresses. Trends Plant Sci. 2019;24 (5):431–442.
19. Wickland DP, Hanzawa Y. The *FLOWERING LOCUS T/ TERMINAL FLOWER 1* gene family: functional evolution and molecular mechanisms. Mol. Plant. 2015;8 (7):983–997.
20. Conti L, Bradley D. *TERMINAL FLOWER 1* is a mobile signal controlling Arabidopsis architecture. Plant Cell. 2007;19 (3):767–778.
21. Flachowsky H, Peil A, Sopanen T, Elo A, Hanke V. Overexpression of *BpMADS4* from silver birch (Betula pendula Roth.) induces early-flowering in apple (Malus aldomestica Borkh.). Plant Breed. 2007;126 (2):137–145.
22. Freiman A, Shlizerman L, Golobovitch S, Yablovitz Z, Korchinsky R, Cohen Y, Samach A, Chevreau E, Roux PM, Patocchi A, Flaishman MA. Development of a transgenic early flowering pear (*Pyrus*

communis L.) genotype by RNAi silencing of *PcTFL1-1* and *PcTFL1-2*. Planta. 2012;235 (6):1239–1251.

23. Luo C, Yu HX, Fan Y, Zhang XJ, He XH. Research advance on the flowering mechanism of mango. Acta Hortic. 2019;1244 (2):17–22.
24. Wei JY, Liu DB, Liu GY, Tang J, Chen YY. Molecular cloning, characterization, and expression of *MiSOC1*: a homolog of the flowering gene *SUPPRESSOR OF OVEREXPRESSION OF CONSTANS1* from mango (*Mangifera indica* L). Front. Plant Sci. 2016;7:1758.
25. Yu HX, Luo C, Fan Y, Zhang XJ, Huang F, Li M, He XH. Isolation and characterization of two *APETALA1-Like* genes from mango (*Mangifera indica* L.). Sci. Hortic. (Amsterdam, Neth.). 2020; 259:108814
26. Fan ZY, He XH, Fan Y, Yu HX, Wang YH, Xie XJ, Liu Y, Mo X, Wang JY, Luo C. Isolation and functional characterization of three *MiFTs* genes from mango. Plant Physiol. Bioch. 2020;155:169–176.
27. Liu Y, Luo C, Zhang XJ, Lu XX, Yu HX, Xie XJ, Fan ZY, Mo X, He XH. Overexpression of the mango *MiCO* gene delayed fowering time in transgenic Arabidopsis. Plant Cell Tissue Organ Cult. 2020;143:219–228.
28. Hanzawa Y, Money T, Bradley D. A single amino acid converts a repressor to an activator of flowering. Proc. Natl. Acad. Sci. USA. 2005;102 (21):7748–7753.
29. Liu B, Watanabe S, Uchiyama T, Kong F, Kanazawa A, Xia Z, Nagamatsu A, Arai M, Yamada T, Kitamura K, Masuta C, Harada K, Abe J, The soybean stem growth habit gene *Dt1* is an ortholog of *Arabidopsis TERMINAL FLOWER 1*. Plant Physiol. 2010;153:198–210.
30. Jiang YY, Zhu YM, Zhang L, Su WB, Peng JR, Yang XH, Song HW, Gao YS, Lin SQ. *EjTFL1* genes promote growth but inhibit flower bud differentiation in loquat. Front. Plant Sci. 2020;11:576.
31. Wu L, Li F, Deng Q, Zhang S, Liu G. Identification and characterization of the *FLOWERING LOCUS T/ TERMINAL FLOWER 1* gene family in petunia. DNA Cell Biol. 2019;38 (9):982–995.
32. Zhang X, Wang C, Pang C, Wei H, Wang H, Song M, Fan S, Yu S, Fang DD. Characterization and functional analysis of PEBP family genes in upland cotton (*Gossypium hirsutum* L.). PLoS ONE. 2016;11 (8):e0161080.
33. Kotoda N, Iwanami H, Takahashi S, Abe K. Antisense expression of *MdTFL1*, a *TFL1-like* gene, reduces the juvenile phase in apple. J. Am. Soc. Hortic. Sci. 2006;131 (1):74–81.
34. Vyavahare SN, Krishna B, Joshi SS, Chaudhari RS, Sane PV. Characterization of mango *Flowering Locus T* (*FT*) and *TERMINAL Flower 1* (*TFL1*) gene. J. Am. Soc. Hortic. Sci. 2017;1183:113–124.
35. Pillitteri LJ, Lovatt CJ, Walling LL. Isolation and characterization of a *TERMINAL FLOWER* homolog and its correlation with juvenility in citrus. Plant Physiol. 2004;135 (3):1540–1551.
36. Chen Y, Jiang P, Thammannagowda S, Liang H, Wilde HD. Characterization of peach *TFL1* and comparison with *FT/ TFL1* gene families of the rosaceae. J. Am. Soc. Hortic. Sci. 2013;138 (1):12–17.

37. Wang Y, Pijut PM. Isolation and characterization of a *TERMINAL FLOWER 1* homolog from Prunus serotina Ehrh. Tree Physiol. 2013;33 (8):855–865.
38. Esumi T, Tao R, Yonemori K. Isolation of *LEAFY* and *TERMINAL FLOWER 1* homologues from six fruit tree species in the subfamily maloideae of the rosaceae. Sex Plant Reprod. 2005;17 (6):277–287.
39. Bi Z, A.T. Tahir, Huang H, Hua Y, Cloning and functional analysis of five *TERMINAL FLOWER 1/CENTRORADIALIS*-like genes from Hevea brasiliensis. Physiol. Plant. 2019;166 (2):612–627.
40. Kotoda N, Wada M. *MdTFL1*, a *TFL1 -like* gene of apple, retards the transition from the vegetative to reproductive phase in transgenic Arabidopsis. Plant Sci. 2005;168 (1):95–104.
41. Gao Y, Gao Y, Wu Z, Bu X, Fan M, Zhang Q. Characterization of *TEMINAL FLOWER 1* homologs *CmTFL1c* gene from Chrysanthemum morifolium. Plant Mol. Biol. 2019;99 (6):587–601.
42. Liu Y, Gao Y, Yuan L, Zhang Q. Functional characterization and spatial interaction of *TERMINAL FLOWER 1* in Hemerocallis. Sci. Hortic. 2019;253:154–162.
43. Miho KS, Rie KI, Chiaki OT, Chojiro K, Misa NF, Izuru O, Hiroyuki T, Ko S, Ken-Ichiro T. TFL1-Like proteins in rice antagonize rice FT-Like protein in inflorescence development by competition for complex formation with 14-3-3 and FD. Plant Cell Physiol. 2018;59 (3):458–468.
44. Niu X, Guan YX, Chen SK, Li HF. Genome-wide analysis of basic helix-loop-helix (bHLH) transcription factors in Brachypodium distachyon. BMC Genom. 2017;18 (1):619.
45. Luo C, He XH, Chen H, Hu Y, Ou SJ. Molecular cloning and expression analysis of four actin genes (*MiACT*) from mango. Biol. Plant. 2013;57 (2): 238–244.
46. Livak KJ, Schmittgen TD. Analysis of Relative Gene Expression Data using Real-Time Quantitative PCR, and the $2^{-\Delta\Delta CT}$ method. Methods. 2002;25 (4):402–408. 2001.
47. Clough SJ, Bent AF. Floral dip: a simplifed method for Agrobacterium- mediated transformation of Arabidopsis thaliana. Plant J. 1998;16 (6):735–743.

Figures

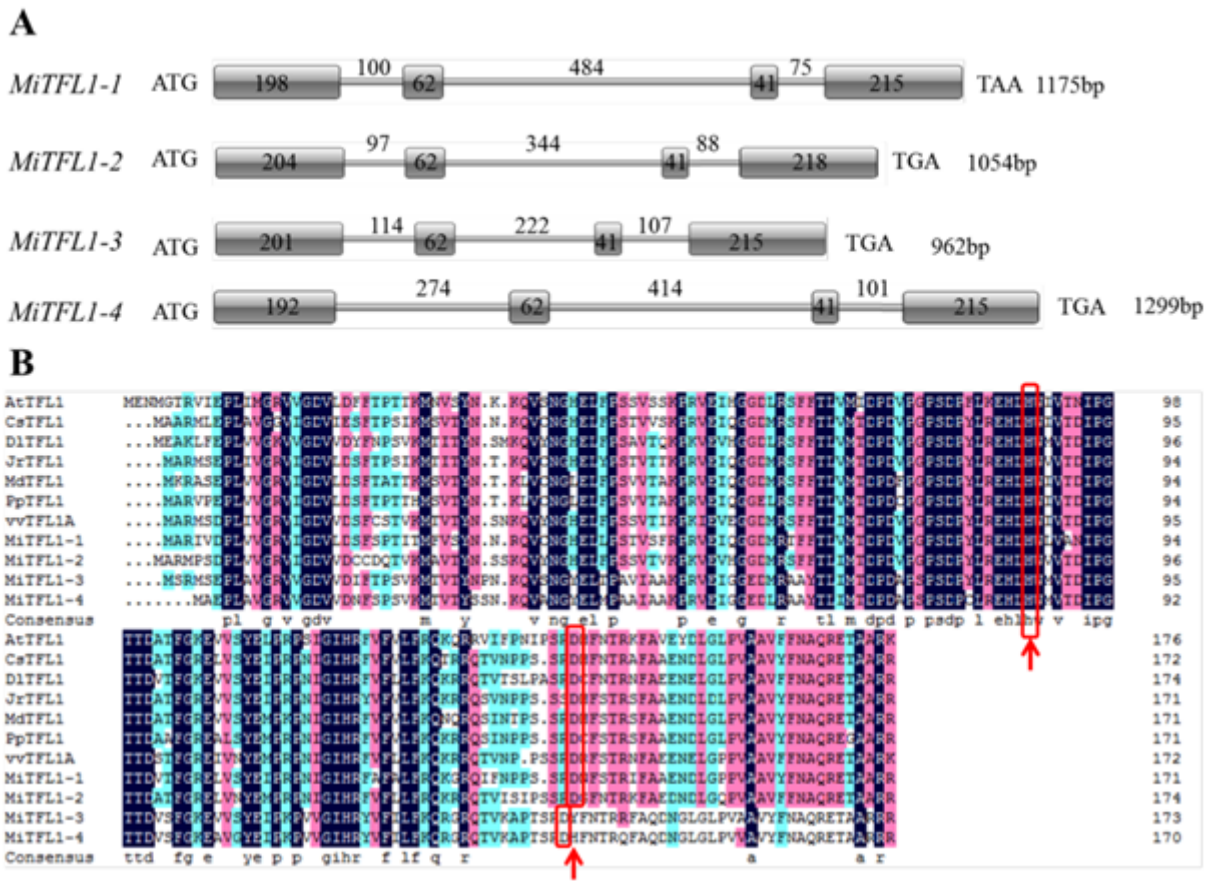

Figure 1

Multiple sequence alignment and gene structure of TFL1 genes. A Gene structures of MiTFL1 genes. B Amino acid sequence alignments of TFL1 proteins from different fruit trees and Arabidopsis thaliana. The following species were included in the analysis (the GenBank accession numbers are shown in parenthesis): Arabidopsis thaliana (AtTFL1, NP_196004.1), Citrus sinensis (CsTFL1, NP_001275848), Dimocarpus longan (DlTFL1, AHY24028.1), Juglans regia (JrTFL1, XP_018811176.1), Malus domestica (MdTFL1, NP_001280887.1), Pyrus x bretschneideri (PpTFL1, NP_001289244.1), and Vitis vinifera (VvTFL1A, NP_001267929.1). The black color indicates that the sequences are exactly the same, the red color indicates ≥75% similarity, and the blue color indicates ≥50% similarity; the red box indicates the key residues His85 and Asp140 of TFL1-like proteins.

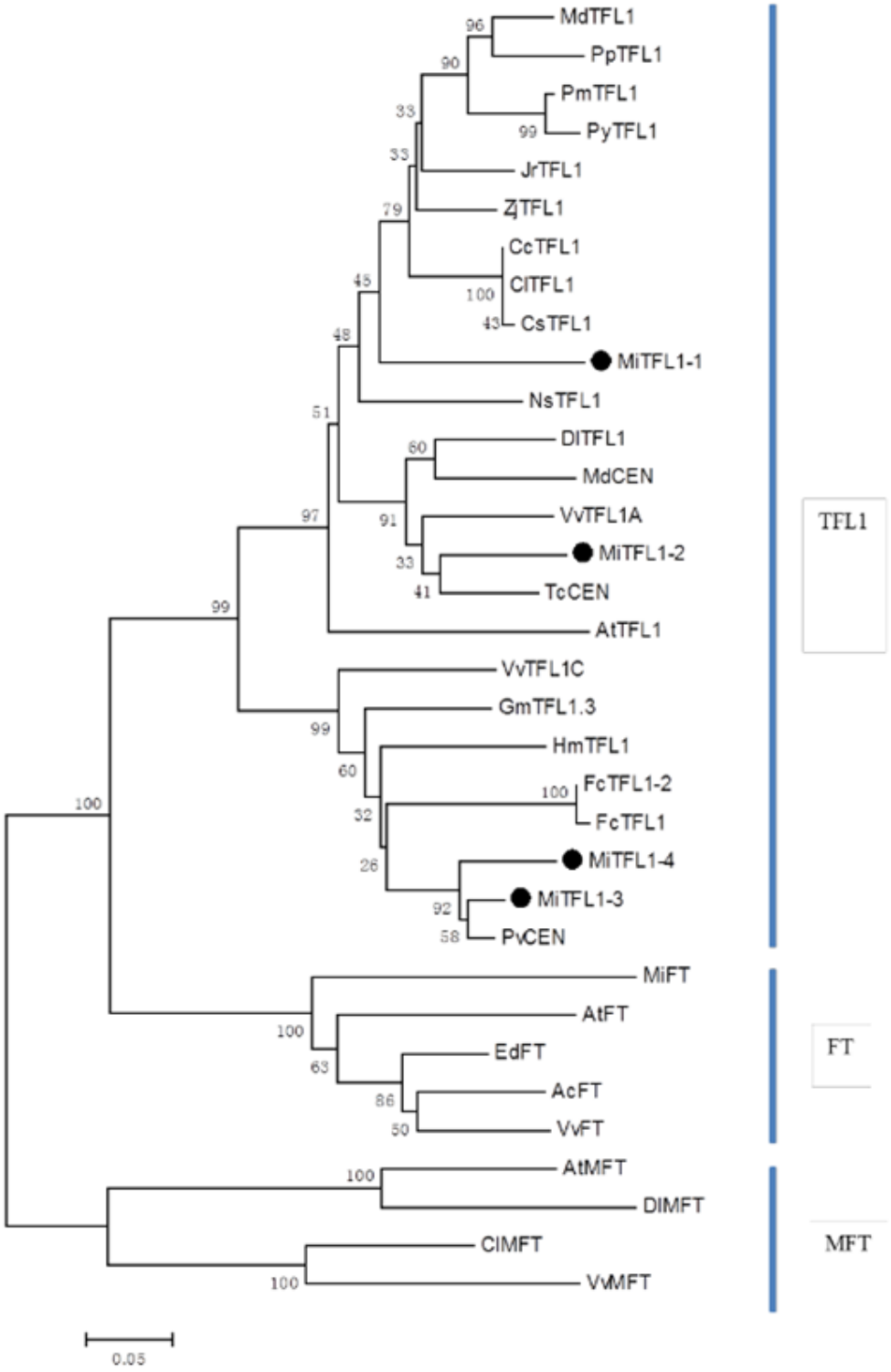

Figure 2

Phylogenetic tree analysis of PEBP proteins. The following species were included in the analysis (the GenBank accession numbers are shown in parenthesis): Arabidopsis thaliana (AtTFL1, NP_196004.1), Citrus sinensis (CsTFL1, NP_001275848), Dimocarpus longan (DlTFL1, AHY24028.1), Juglans regia (JrTFL1, XP_018811176.1), Malus domestica (MdTFL1, NP_001280887.1), Pyrus x bretschneideri (PpTFL1, NP_001289244.1), Malus domestica (MdCEN, NP_001280940.1), Pistacia vera (PvCEN protein

1, XP_031269481.1), Theobroma cacao (TcCEN, XP_017973069.1), Hydrangea macrophylla (HmTFL1, MF374628.1), Glycine max (GmTFL1.3, FJ573238.1), Ficus carica (FcTFL1-2, AB746842.1), Citrus clementina (CcTFL1, XP_006430226.1), Citrus limon (ClTFL1, AWW25018.1), Ficus carica (FcTFL1, BAX00857.1), Nicotiana sylvestris (NsTFL1, XP_009766168.1), Prunus mume (PmTFL1, AEO72021.1), Prunus yedoensis (PyTFL1, AEO72023.1), Vitis vinifera (VvTFL1A, NP_001267929.1), Vitis vinifera (VvTFL1C, NP_001267933.1), Ziziphus jujube (ZjTFL1, XP_015898753.1), Actinidia chinensis (AcFT, AJA40932.1), Arabidopsis thaliana (AtFT, BAA77838.1), Eriobotrya deflexa (EdFT, AMB72867.1), Mangifera indica (MiFT, AGA19021.1), Vitis vinifera (VvFT, NP_001267907.1), Arabidopsis thaliana (AtMFT, OAP13671.1), Citrus limon (ClMFT, AWW25016.1), Dimocarpus longan (DlMFT, AUG98253.1), and Vitis vinifera (VvMFT, NP_001267935.1).

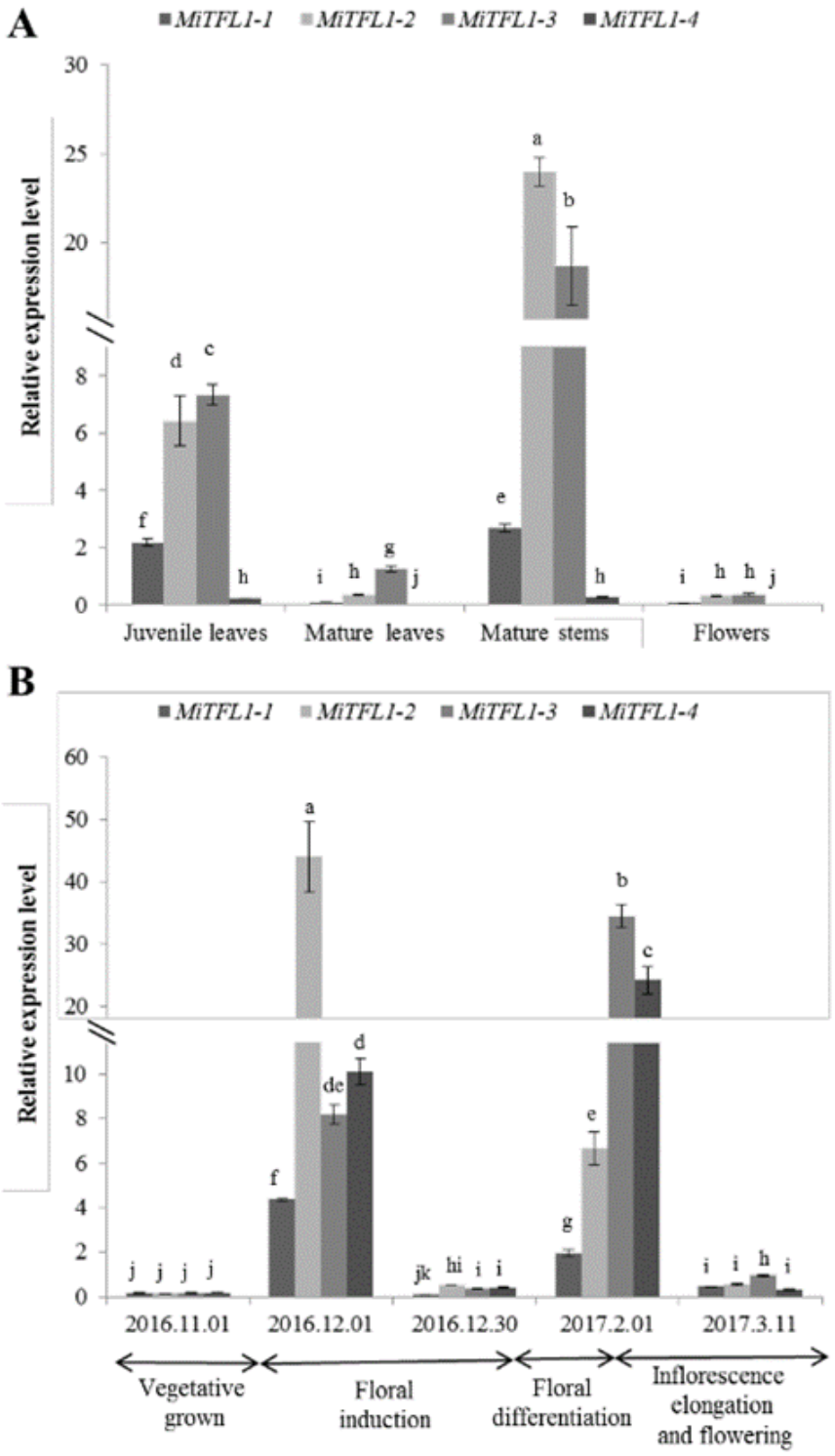

Figure 3

qRT-PCR analysis of the expression profile of MiTFL1s in mango. The significance of the differences among the samples was assessed by Student's t-tests ($P < 0.05$). A Expression pattern of MiTFL1 genes in various tissues (juvenile leaves, mature leaves, mature stems, and flowers). B Expression pattern of MiTFL1 genes in mature leaves over time.

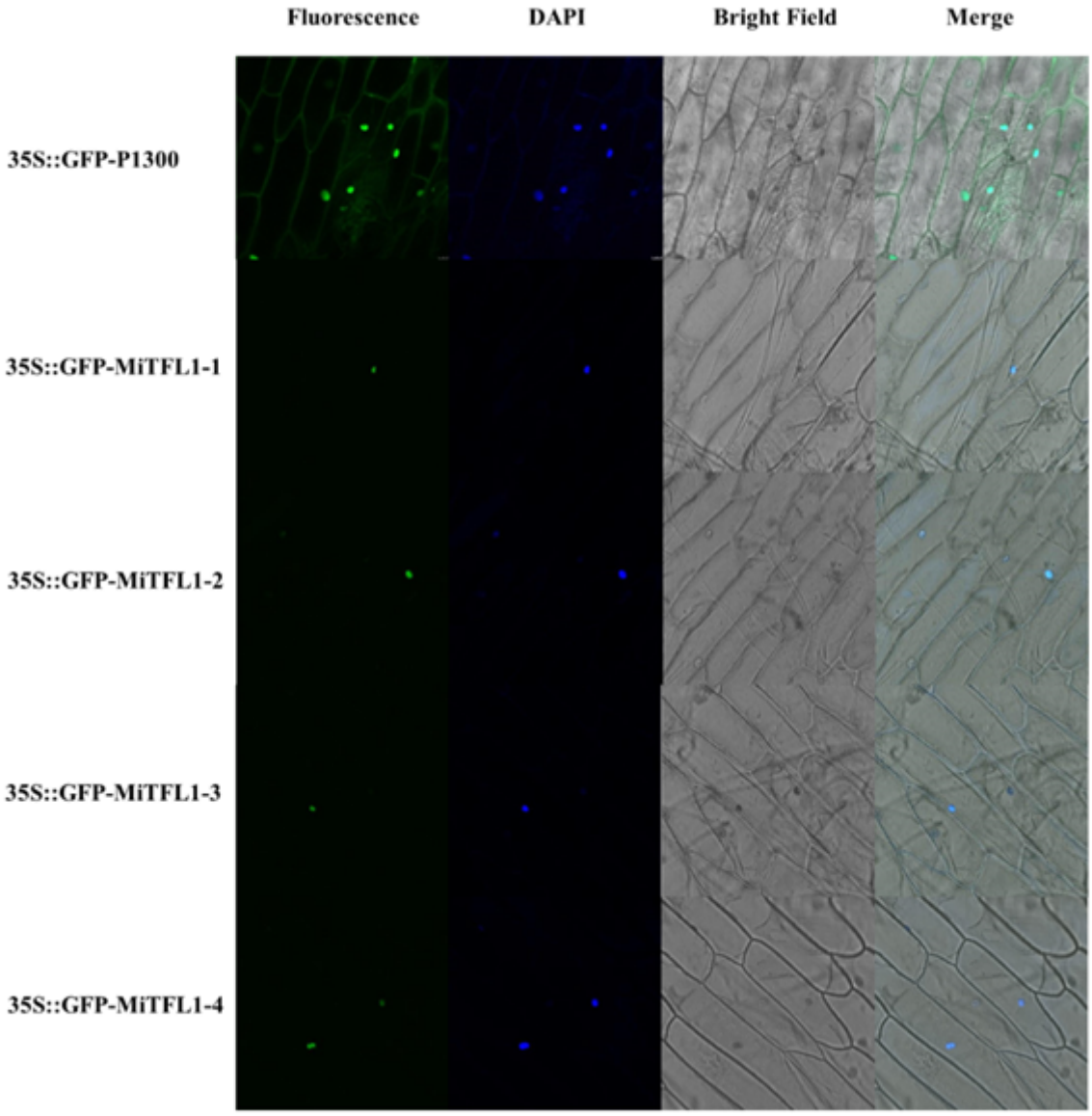

Figure 4

Subcellular localization analysis of MiTFL1s. 35S::GFP-P1300 and 35S::GFP- MiTFL1s were localized in onion epidermal cells.

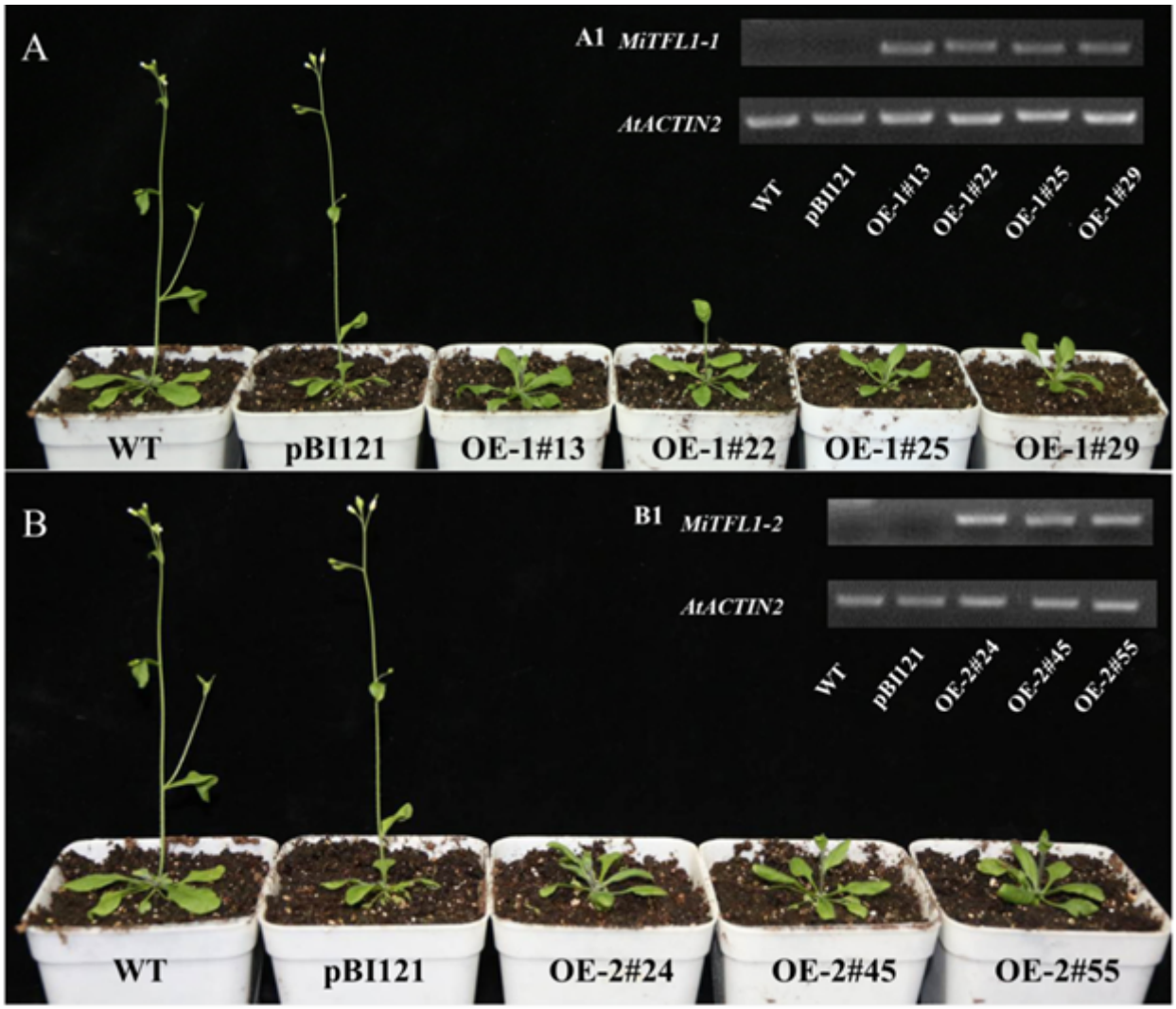

Figure 5

Phenotype of transgenic Arabidopsis lines and expression profiles of the transgenes. A Phenotype of MiTFL1-1-overexpressing transgenic lines showing delayed flowering (right) and of WT and pBI121 transgenic lines as controls (left) under LD conditions. A1 RT-PCR analysis of MiTFL1-1 in the control and MiTFL1-1-overexpressing transgenic lines. B Phenotype of MiTFL1-2 -overexpressing transgenic lines showing delayed flowering (right) and of the WT and pBI121 transgenic lines as controls (left) under LD conditions. B1 RT-PCR analysis of MiTFL1-2 in the control and MiTFL1-2-overexpressing transgenic lines. The original data can be viewed from Additional file 2: Fig. S1a-b.

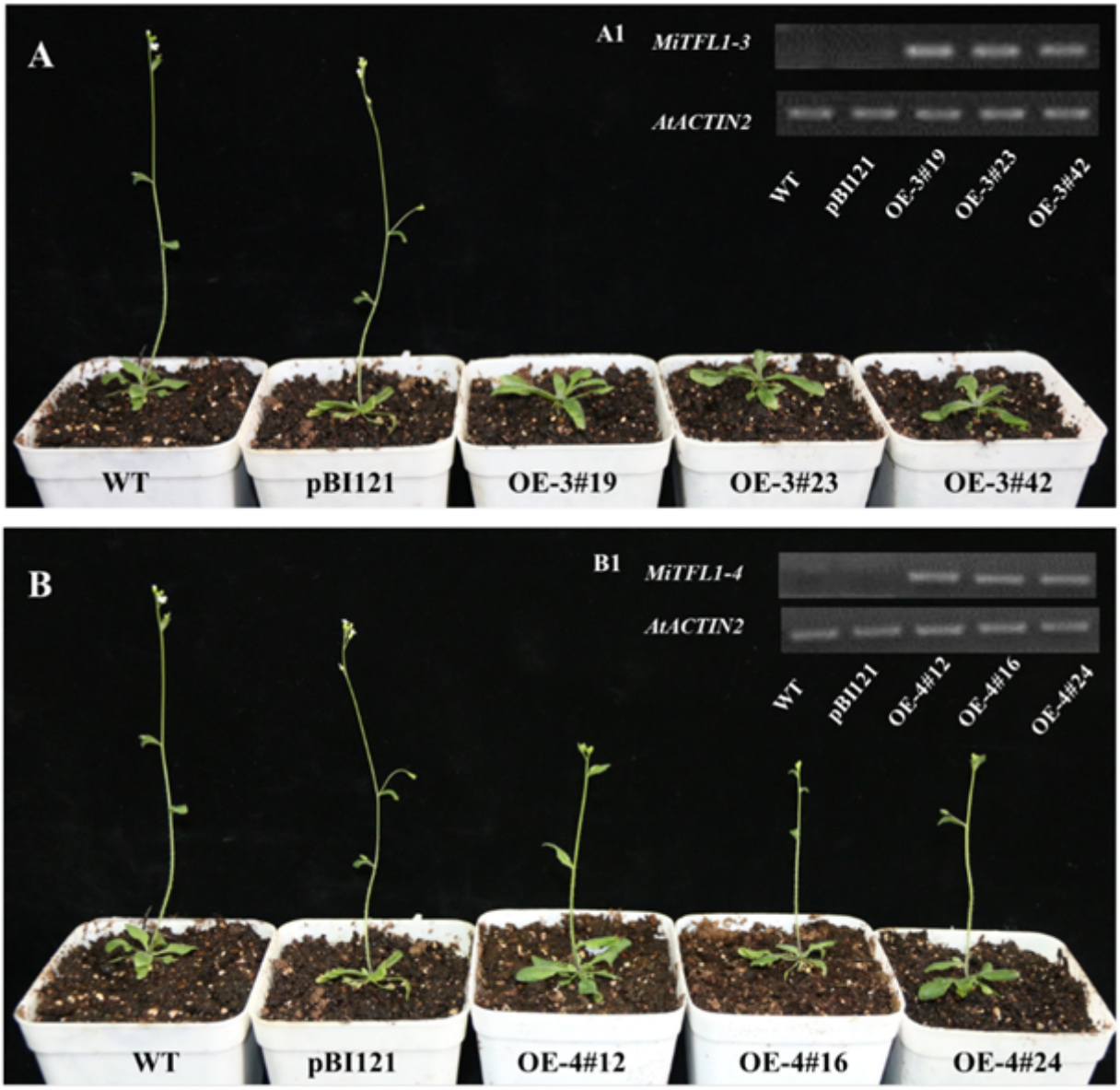

Figure 6

Phenotype of transgenic Arabidopsis lines and expression profiles of the transgenes. A Phenotype of MiTFL1-3-overexpressing transgenic lines showing delayed flowering (right) and of WT and pBI121 transgenic lines as controls (left) under LD conditions. A1 RT-PCR analysis of MiTFL1-3 in the control and MiTFL1-3-overexpressing transgenic lines. B Phenotype of MiTFL1-4 -overexpressing transgenic lines showing delayed flowering (right) and of the WT and pBI121 transgenic lines as controls (left) under LD conditions. B1 RT-PCR analysis of MiTFL1-4 in the control and MiTFL1-4-overexpressing transgenic lines. The original data can be viewed from Additional file 2: Fig. S1c-d.

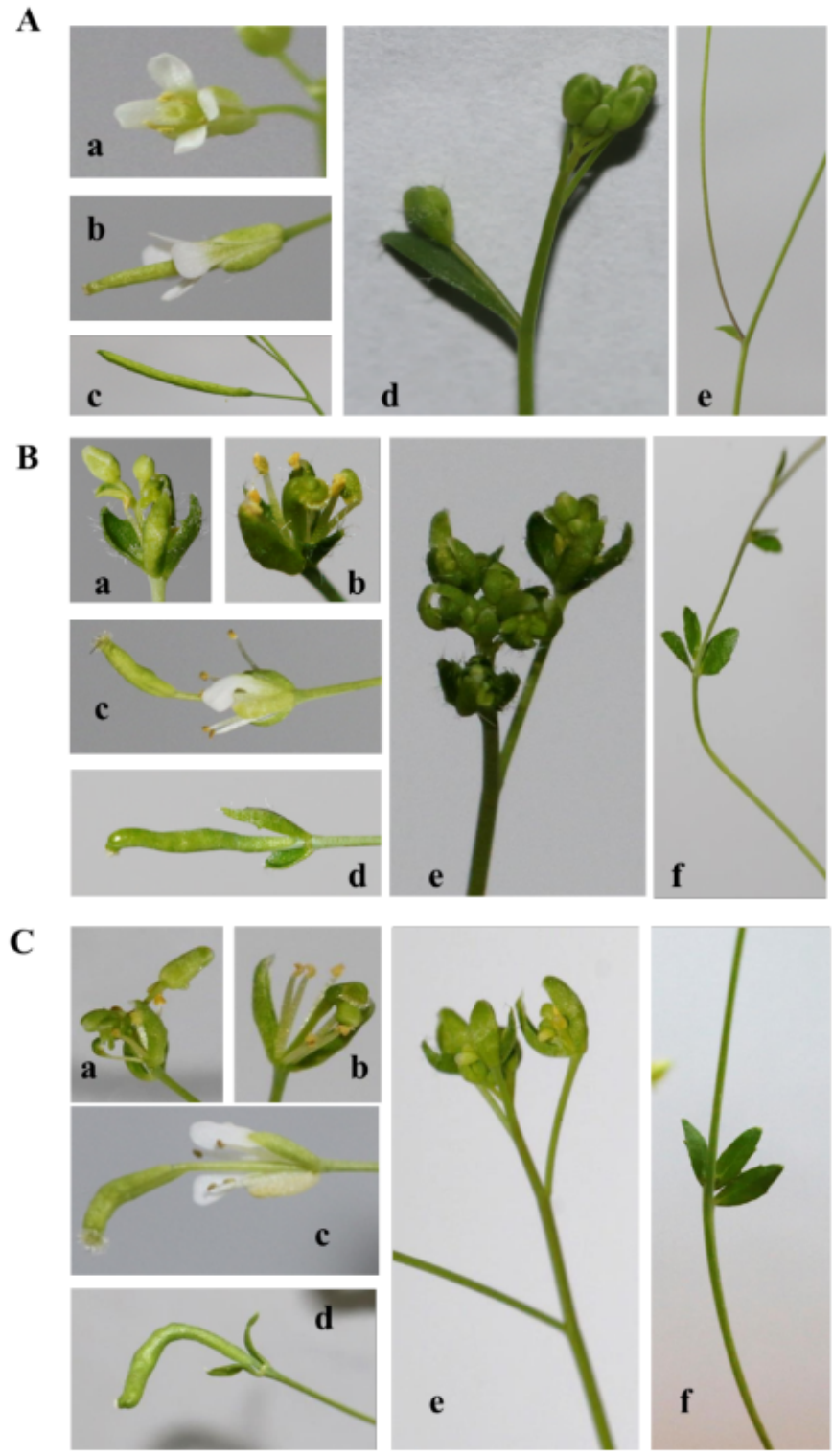

Figure 7

Photographs of plant architecture, inflorescence, and floral phenotypes of WT and MiTFL1-1 and MiTFL1-3 transgenic Arabidopsis lines. A Phenotypes of WT Arabidopsis: (a, b) flowers, (c) silique, (d) inflorescence, and (f) stem. B Phenotypes of MiTFL1-1-overexpressing line OE-1#13: (a) the flower organs are changed, and no petals or carpels turned into a new inflorescence; (b) flower lacking petals; (c) a longer pod stalk that formed in flowers; (d) pods showing curved growth; (e) abnormal inflorescence; and

(f) whorled leaves growing on the stem. C Phenotypes of MiTFL1-3-overexpressing line OE-3#19: (a) flower organs are altered, and no petals or carpels turned into a new inflorescence; (b) flower lacking petals; (c) a longer pod stalk that formed in flowers; (d) pods showing curved growth; (e) abnormal inflorescence; and (f) whorled leaves growing on the stem.

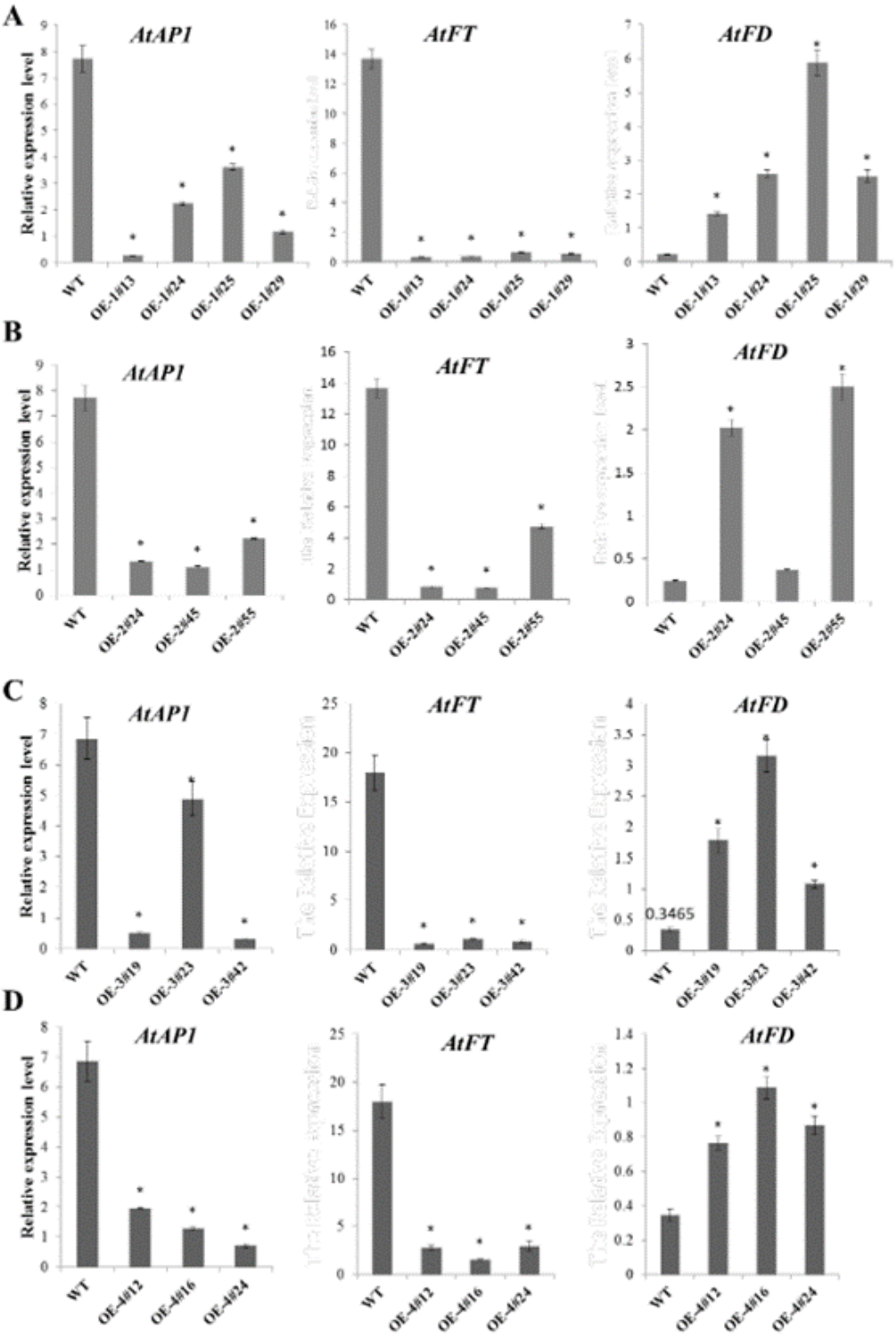

Figure 8

Expression analyses of flowering-related genes in transgenic Arabidopsis. A-D qRT-PCR analysis of endogenous flowering-related genes, including Arabidopsis AtAP1, AtFT and AtFD, in the MiTFL1s-overexpressing and WT lines, respectively. The expression level was normalized to that of Arabidopsis AtACTIN2. The data are shown as the means ± SEs from three biological replicates. The significance of the differences among the samples was determined by Duncan's test ($P < 0.05$).

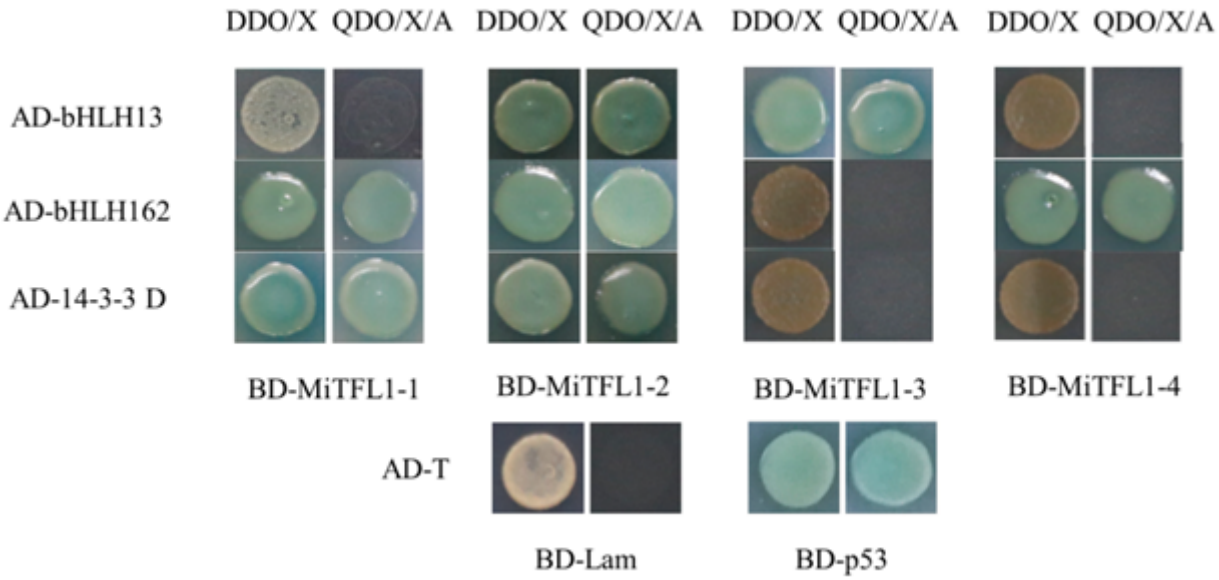

Figure 9

Identification of interactions between MiTFL1s and other proteins in yeast. The interacting proteins were obtained through library screening; pGBKT7-53 and pGADT7-T served as positive controls, and pGBKT7-Lam and pGADT7-T were used as negative controls. The strains were cultured on DDO/–Trp/–Leu/X-α-gal (200 ng/ml) and QDO/–Trp/–Leu/–His/–Ade/X-α-gal (200 ng/ml)/AbA (500 μg/ml) medium.

Supplementary Files

This is a list of supplementary files associated with this preprint. Click to download.

- FigureS1.docx
- FigureS2.docx
- SupplementaryTable.1.xlsx